Equilibrium array configurations with respect to the deviatoric mean drift forces

Grgur Tokić & Dick K.P. Yue
gtokic@mit.edu yue@mit.edu

Department of Mechanical Engineering
Massachusetts Institute of Technology, Cambridge MA 02139, USA

Introduction

The mean drift force (MDF) acting on a floating structure plays an important role in the design of offshore systems. Usually the primary focus is the total downwave MDF on an entire structure as it determines the mooring system. If a structure consists of a number of elements, the MDF acting on an each element is configuration dependent and not purely in the downwave direction, but, due to the multiple wave interactions occurring among the elements, it also has a component perpendicular to the wave direction. For offshore systems consisting of individually moored floating structures, e.g. wave energy converter arrays or floating wind farms, the differences in the MDF acting on individual structures can lead to a change of the spatial configuration of the array and significantly alter the first-order system response.

The mean drift force on structures has been studied for a long time [1–4]. The focus on the total downwave MDF is reflected in the number of recent studies on the so-called cloaking [5–8], where the goal is to eliminate the downwave MDF by surrounding a "target" body with scatterers. The effects of the differences in the MDF acting on the individual bodies in these arrays were not studied.

Recently, Tokić and Yue [9] considered the so-called deviatoric mean drift forces in line arrays oriented normally to the incident flow. They studied the equilibrium configurations of these line arrays with respect to the deviatoric MDFs that act in the direction of the array axis, i.e. they obtained equilibrium configurations of arrays constrained to remain in line. They showed that the deviatoric MDFs on each body are significant (on the order of the downwave MDF on an isolated body) but that they cancel out in equilibrium configurations.

Here, we look for true equilibrium configurations with respect to the deviatoric MDFs, i.e. those for which *all* components of the deviatoric MDFs are zero, and we discuss their stability with respect to the configuration perturbations.

Problem Formulation

We consider arrays $\mathcal{A}_N$ of N fixed vertical bottom-mounted circular cylinders of radius a in a fluid of constant depth h. The position $\boldsymbol{x}_j$ of body $\mathcal{B}_j$ in an array is $\boldsymbol{x}_j = (x_j, y_j)$, $j = 1, \ldots, N$. The spatial configuration $\mathcal{C}(\boldsymbol{b})$ of $\mathcal{A}_N$ is, in general, described in terms of P configuration parameters $\boldsymbol{b} = (b_1, \ldots, b_P)$, where $P \leq 2(N-1)$. We consider monochromatic waves (angular frequency ω, wavenumber k, amplitude A) incident on the array in the context of linear potential theory (potential $\varPhi = \mathrm{Re}(\phi\, \mathrm{e}^{-\mathrm{i}\omega t})$), Fig. 1.

The mean drift force $\boldsymbol{D}_j(kh; \mathcal{C}) = (X_j, Y_j)$ on a body $\mathcal{B}_j$ in an array ($j = 1, \ldots, N$) is a time-constant nonlinear, second-order hydrodynamic force that is fully determined by the first-order potential ϕ

$$\boldsymbol{D}_j = \frac{\rho}{4} \iint_{\mathscr{S}_j} |\nabla\phi|^2 \, \boldsymbol{n}_\mathrm{H} \, dS - \frac{\rho\,\omega^2}{4g} \oint_{\mathscr{C}_j} |\phi|^2 \, \boldsymbol{n}_\mathrm{H} \, dl \, , \tag{1}$$

where $\mathscr{S}_j$ is the mean wetted surface and $\mathscr{C}_j$ the mean waterline of $\mathcal{B}_j$, and $\boldsymbol{n}_\mathrm{H}$ is the horizontal projection of the surface normal $\boldsymbol{n}$ (pointing into the fluid). In general, the differences between $\boldsymbol{D}_j$ acting on different bodies in the array would, if the bodies were not fixed, act to displace the bodies relative to each other. Relative to a reference mean drift force $\boldsymbol{D}_\mathrm{r} \equiv \boldsymbol{D}_1$, we define the deviatoric mean drift force

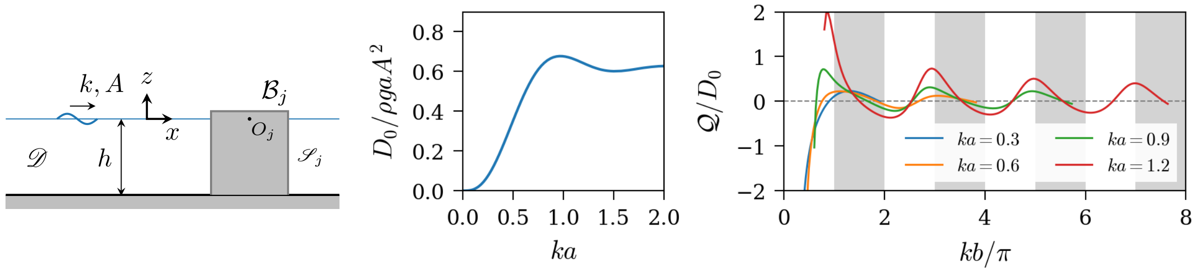

Figure 1: **Left:** Side view of the problem domain. **Center:** Mean drift force D_0 on a bottom-mounted isolated vertical cylinder (radius $a/h = 0.3$). **Right:** Normalized deviatoric force $\mathcal{Q} \equiv |Y_1 - Y_2|$ in 2-body arrays normally oriented to the incident wave as a function of inter-body spacing b [9].

$\boldsymbol{\mathcal{D}}_i(kh; \mathcal{C}) \equiv \boldsymbol{D}_{i+1} - \boldsymbol{D}_\mathrm{r}$, $i = 1, \ldots, N-1$. While the MDF on an isolated cylinder $D_0(kh)$ is in the direction of wave propagation and is strictly positive, $\boldsymbol{\mathcal{D}}_i$ generally has a non-zero component in the cross-wave direction (i.e. perpendicular to the direction of propagation of the incident wave) due to the wave interactions occurring in the array. For example, the deviatoric mean force occurring in 2-body arrays normally oriented to the incident wave oscillates around zero (with $O(1)$ magnitude), indicating an infinite number of equilibrium configurations [9], Fig. 1. For convenience, we collect all $\boldsymbol{\mathcal{D}}_i$ in a single deviatoric force vector $\boldsymbol{\mathcal{Q}}$.

We define an equilibrium configuration $\mathcal{C}^* \equiv \mathcal{C}(\boldsymbol{b}^*)$, associated with the equilibrium configuration parameters $\boldsymbol{b}^*$, as the configuration for which $\boldsymbol{\mathcal{Q}}(kh; \boldsymbol{b}^*) = \boldsymbol{0}$. The equilibrium configurations $\mathcal{C}^*$ would not be affected by deviatoric forces even if the bodies were free to move. For a given incident wave, $\mathcal{A}_N$ generally has many equilibrium configurations $\mathcal{C}^{*,j}$ (corresponding to equilibrium configuration parameters $\boldsymbol{b}^{*,j}$, $j = 1\ldots$). The stability of $\mathcal{C}^*$ can be assessed by considering configurations $\mathcal{C}(\boldsymbol{b})$ in the neighborhood of $\boldsymbol{b}^*$, i.e. the eigenvalues $\boldsymbol{\lambda}$ of the Jacobian $\partial\boldsymbol{\mathcal{Q}}/\partial\boldsymbol{b}$ at $\boldsymbol{b}^*$. An equilibrium configuration $\mathcal{C}^*$ is stable if the real parts of all the eigenvalues are negative ($\mathrm{Re}(\lambda_i) < 0$, $i = 1, \ldots, P$). Importantly, all the deviatoric forces $\boldsymbol{\mathcal{Q}}(\boldsymbol{b})$ are calculated for fixed configurations $\mathcal{C}(\boldsymbol{b})$, i.e. for zero mean body velocity.

The total complex potential ϕ is obtained using an exact multiple scattering wave-body interaction model [10, 11], which expresses ϕ in terms of the incident and the scattered waves at each body using the partial waves expansion. Enforcing the diffraction boundary condition $\partial\phi/\partial n = 0$ on every $\mathcal{B}_p$ in the array leads to a linear system for the unknown vector of complex amplitudes $\boldsymbol{c}_p$ of the scattered partial waves

$$\sum_{j=1}^{N} \left[\delta_{jp} - (1-\delta_{jp})\,\mathbf{T}_j\,\mathbf{S}_{jp}^\mathrm{T}\right]\boldsymbol{c}_j = \mathbf{T}_p\,\boldsymbol{d}_p^\mathrm{I}\,, \quad p = 1, \ldots, N\,, \tag{2}$$

where $\mathbf{T}_j$ is the diffraction transfer matrix obtained for a body in isolation; δ_{jp} is the Kronecker delta and $(\cdot)^\mathrm{T}$ denotes matrix transpose. The effect of array configuration is expressed solely through the separation matrix $\mathbf{S}_{jp}(\mathcal{C})$, which depends only on the relative positions of the bodies $\mathcal{B}_j$ and $\mathcal{B}_p$. The size of the system $M = N \times N_w$ depends on the number of bodies and the total number of partial waves N_w. The expression (2) is in principle exact (other than the truncation to N_w partial waves), i.e. the full diffraction problem is taken into account, including the effects of evanescent waves.

Once the multiple scattering problem (2) is solved, (1) can be expressed as $D_\xi^p = \boldsymbol{c}_p^\mathrm{H}\,\mathbf{F}_\xi^p\,\boldsymbol{c}_p$, where D_ξ^p is the MDF on $\mathcal{B}_p$ in ξ-direction ($D_x^p \equiv X_p$, $D_y^p \equiv Y_p$), $\mathbf{F}_\xi^p$ is the configuration-independent MDF quadratic transfer matrix in the ξ-direction calculated for a body in isolation, $\boldsymbol{c}_p$ are the scattered wave coefficients for $\mathcal{B}_p$, and $(\cdot)^\mathrm{H}$ denotes the Hermitian transpose [9]. Note that since we require $\boldsymbol{D}_j$ on each body rather than a whole structure, the far-field methods, which calculate the MDF on a whole structure, are not applicable here [4].

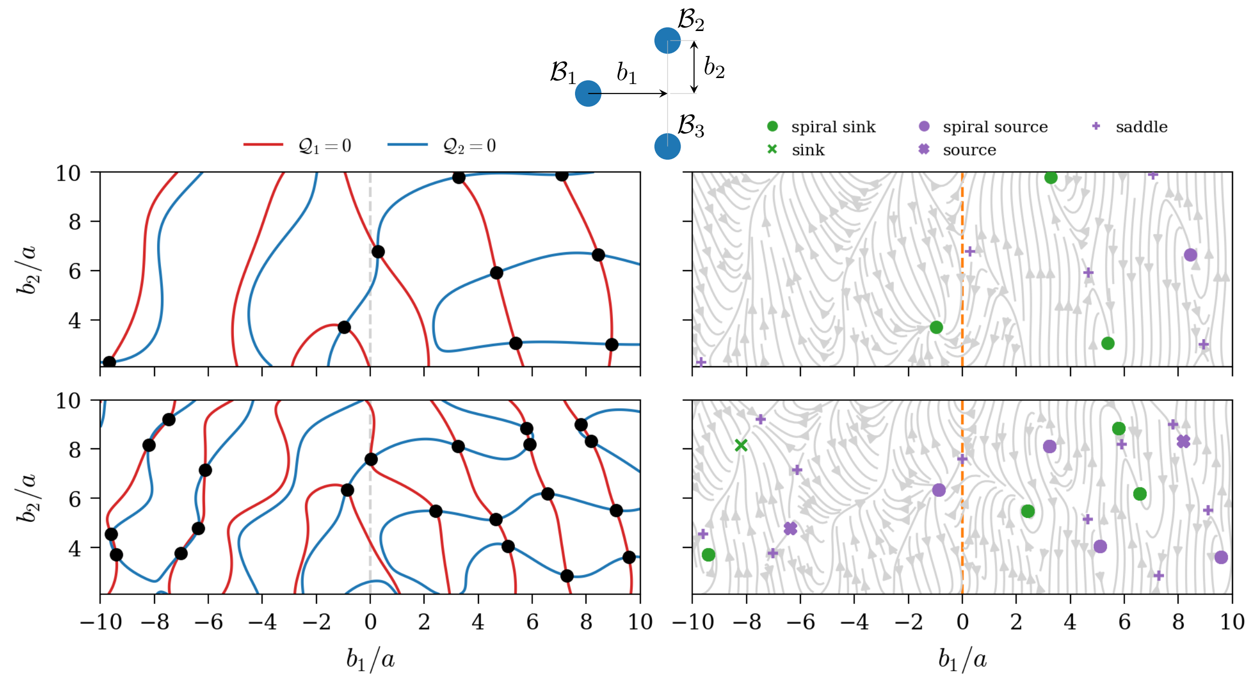

Figure 2: **Left:** The isosceles equilibrium configurations $\mathcal{C}^{*,i}$ of 3-body arrays. **Right:** The phase portrait representation of $\boldsymbol{\mathcal{Q}}$. The stability of $\mathcal{C}^{*,i}$ is indicated with the corresponding symbol (symbols in green correspond to stable $\mathcal{C}^{*,i}$, purple for unstable; see legend). **Top row:** $ka = 0.45$; **bottom row:** $ka = 0.75$.

Results and Discussion

We first look for equilibrium configuration of 3-body arrays that are symmetric with respect to the incident wave direction. While general 3-body arrays require four parameters to define the spatial configuration, these isosceles configurations can be described using only two parameters $\boldsymbol{b} = (b_1, b_2)$. Here we choose $b_1 = x_2$ and $b_2 = y_2$. Due to the symmetry, only two deviatoric force components $\mathcal{Q}_1 = X_2 - X_1$ and $\mathcal{Q}_2 = Y_2 - Y_1$ need to be zero for $\boldsymbol{\mathcal{Q}} = \mathbf{0}$ for equilibrium configurations.

The equilibrium configurations $\mathcal{C}^{*,j}$ can be obtained by considering intersections of $\mathcal{Q}_1 = 0$ and $\mathcal{Q}_1 = 0$ contours in (b_1, b_2) space, Fig. 2. Despite the configuration class constraints, the resulting equilibrium configurations are general and unconstrained because all components of the full deviatoric force vector $\boldsymbol{\mathcal{Q}}$ are zero. This is in contrast to the class-preserving equilibrium configurations of line arrays found in [9], where the equilibrium was defined with respect to only the inline components of deviatoric force. With the increase in wavenumber kh, $\mathcal{C}^{*,j}$ become more dense in (b_1, b_2) space. For a fixed kh, $\mathcal{C}^{*,j}$ are more dense, in general, when the apex of the isosceles configuration is facing the incident wave ($b_1 > 0$).

The stability of equilibrium configurations $\mathcal{C}^{*,j}$ with respect to the class-preserving perturbations $\Delta\boldsymbol{b} = (\Delta b_1, \Delta b_2)$ of isosceles configurations is shown in Fig. 2. Since the configuration parameters and the deviatoric forces both have only two independent components, we can further classify the stability of equilibria depending on the shape of the phase portrait (i.e. the trace and the determinant of the Jacobian $\partial\boldsymbol{\mathcal{Q}}/\partial\boldsymbol{b}$). The obtained equilibria can be both stable and unstable, with the relative number of unstable $\mathcal{C}^{*,j}$ increasing with kh. For lower kh, $\mathcal{C}^{*,j}$ are either saddles or spiral sources and sinks, while pure sources and sinks appear for larger kh.

If the constraint to allow only for class-preserving perturbations is released, the stability character of equilibrium configurations, in general, changes. The stability of $\mathcal{C}^{*,j}$ under independent $(\Delta x_j, \Delta y_j)$ perturbations of each body is given in Fig. 3. Compared to the class-preserving perturbations, the relative number of stable $\mathcal{C}^{*,j}$ is decreased in this case. While there are still stable and unstable $\mathcal{C}^{*,j}$, some of them have changed sign. We only specify general stability character of $\mathcal{C}^{*,j}$ under general perturbations since the two-dimensional phase portraits of $\mathcal{C}^{*,j}$ are not applicable in the higher-dimensional case.

This has practical implications for individually moored $\mathcal{A}_3$ arrays as they are likely to undergo MDF-

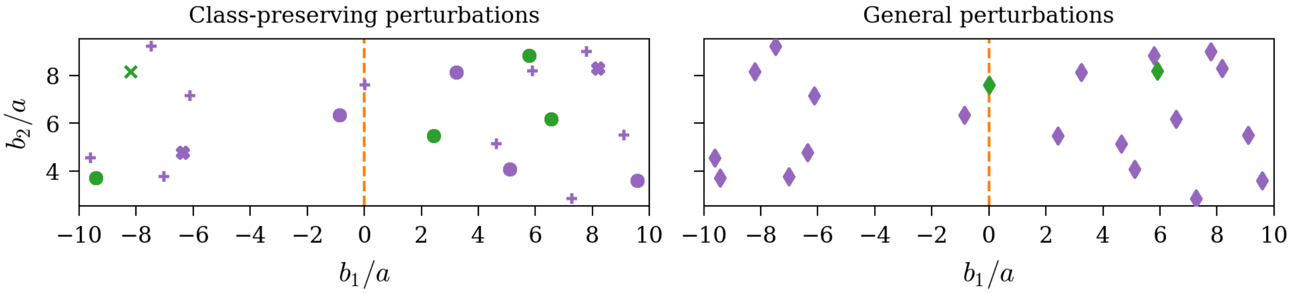

Figure 3: Stability of isosceles equilibrium configurations $\mathcal{C}^{*,j}$ at $ka = 0.75$. **Left:** stability with respect to the class-preserving configuration perturbations (same as in Fig. 2, with corresponding symbols). **Right:** stability with respect to the general body position perturbations (green: stable; purple: unstable).

caused reconfigurations not constrained by any particular configuration class. As a result, they are likely to converge to the equilibria that are stable with respect to general perturbations. We note that the difference in the total downwave mean drift force among isosceles configurations studied here can be as large as ±50%, so individually moored multi-body structures should take into account that the design mean drift force load can significantly change if the array equilibrium is not stable with respect to deviatoric mean drift forces.

As the number of bodies N in an array grows, the only equilibrium configurations are those that satisfy $\boldsymbol{\mathcal{D}}_j = \mathbf{0}$, $j = 1, \dots, N-1$, i.e. the fully unconstrained cases. Special configuration classes of larger arrays, i.e. those where the number of configuration parameters $P < 2 \times (N-1)$, lead to overdetermined systems so there are no class-preserving equilibrium configurations. However, the equilibrium configurations for general unconstrained arrays still exist.

References

[1] H. Maruo. "The drift of a body floating on waves". *Journal of Ship Research* 4 (1960), pp. 1–10.

[2] J. N. Newman. "The Drift Force and Moment on Ships in Waves". *Journal of Ship Research* 11 (01) (1967), pp. 51–60.

[3] G. Thomas. "The diffraction of water waves by a circular cylinder in a channel". *Ocean Engineering* 18 (1-2) (1991), pp. 17–44.

[4] M. Kashiwagi. "Theoretical Study on Wave-Induced Pressure and Drift Force on a Vertical Circular Column". *J. of the Japan Society of Naval Architects and Ocean Engineers* 37 (2023), pp. 37–45.

[5] J. N. Newman. "Cloaking a circular cylinder in water waves". *European Journal of Mechanics - B/Fluids* 47 (2014), pp. 145–150.

[6] T. Iida, M. Kashiwagi, and G. He. "Numerical confirmation of cloaking phenomenon on an array of floating bodies and reduction of wave drift force". *Int. J. of Offshore & Polar Eng.* 24 (2014).

[7] G. Dupont et al. "Cloaking a vertical cylinder via homogenization in the mild-slope equation". *Journal of Fluid Mechanics* 796 (2016).

[8] Z. Zhang et al. "Numerical and experimental studies on cloaked arrays of truncated cylinders under different wave directions". *Ocean Engineering* 183 (2019), pp. 305–317.

[9] G. Tokić and D. K. P. Yue. "Equilibrium configurations of line arrays with respect to the deviatoric mean drift forces" (under review).

[10] H. Kagemoto and D. K. P. Yue. "Interactions among multiple three-dimensional bodies in water waves: an exact algebraic method". *Journal of Fluid Mechanics* 166 (1986), pp. 189–209.

[11] G. Tokić and D. K. P. Yue. "Hydrodynamics of periodic wave energy converter arrays". *Journal of Fluid Mechanics* 862 (2019), pp. 34–74.